

## Determination of ice-shelf bottom melting by time-domain reflectometry

K. GROSFELD AND N. BLINDOW

*Institut für Geophysik, Forschungsstelle für physikalische Glaziologie der Westfälischen Wilhelms-Universität Münster, D-4400 Münster, Germany*

**ABSTRACT.** For our work in the Filchner-Ronne Ice Shelf Programme (FRISP), we have developed a new technique for measuring the bottom-melting rate with high reliability. The method is based on time-domain reflectometry (TDR) measurements of transmission lines inserted into melt holes. The TDR-data are digitally recorded on magnetic tape. System resolution has been estimated at 0.2 m. Hence, re-measuring after 1 year gives an accuracy of 10% for melting rates of  $2 \text{ m a}^{-1}$ . Two transmission lines for TDR measurements were installed during the German FRIS Expedition 1989–90. This paper describes the design of the system. Examples of recorded wave forms are given.

### INTRODUCTION

Bottom melting is a significant parameter for the mass balance of ice shelves. Up to now, this quantity has been estimated by modeling or calculated from velocity, thickness and its gradient, accumulation rate and strain under the assumption of steady-state conditions (Crary and others, 1962). To our knowledge, no attempt to obtain an independent determination of the bottom-melting rate has been made so far.

During the German Antarctic Expedition 1989–90 on the Filchner-Ronne Ice Shelf (FRIS), hot-water drilling was undertaken at  $77^\circ \text{ S}$ ,  $52.3^\circ \text{ W}$  to investigate the basal marine-ice layer in the central part of the FRIS. This feature was discovered and described by Thyssen (1988). The hot-water drilled holes pierced the ice shelf several times. The holes were used mainly to insert chains with Pt100 elements to measure the temperature–depth profile down to the bottom of the ice shelf. The access to the sea beneath the ice was used for water sampling and the installation of a current meter.

An almost complete set of glaciological data from core drillings, radio-echo sounding, field glaciology and geodetic work is available for the investigated area. The only unknown parameter for the calculation of mass balance is the basal melting rate in this area. Hence, we designed a simple experimental set-up for the measurement of basal melting. This measurement is independent of the assumption of steady-state flow. By comparing measured and calculated values, one can estimate whether or not the ice shelf is in a steady state.

### METHOD

Time-domain reflectometry (TDR) is a method normally used to detect faults on transmission lines by transmitting a short pulse that is reflected at impedance discontinuities.

From the travel time of the reflected pulses and the propagation velocity along the cable, the distance to the fault is calculated. The impedance of a parallel transmission line is dependent on the dielectric properties of its surroundings. Thus, it can be used as a sensor for dielectric discontinuities. This technique has been applied for the determination of soil water content (Topp and others, 1982a, b; Blindow and others, 1987) and to investigate the dielectric properties of sea ice (Morey and others, 1984).

A prominent dielectric discontinuity is the ice/sea-water boundary. If a parallel transmission line frozen into the ice shelf protrudes into the sea water, an incident pulse will be reflected with an amplitude reflection coefficient of  $-0.93$  at the ice-shelf bottom. Since it is impractical to freeze bare parallel wires into the ice, we used a standard  $240 \Omega$  strip line. The polyethylene insulation of this unshielded cable is only 0.55 mm thick, so the propagation constant of the cable is still influenced by the surrounding dielectric.

The propagation velocities along the cable immersed in different media were determined by TDR laboratory experiments. The results are  $143 \pm 2 \text{ m } \mu\text{s}^{-1}$  for tap water,  $141 \pm 2 \text{ m } \mu\text{s}^{-1}$  for sea water (NaCl solution: 35‰),  $194 \pm 2 \text{ m } \mu\text{s}^{-1}$  for ice and  $245 \pm 2 \text{ m } \mu\text{s}^{-1}$  for air.

From the velocities, reflection coefficients can be calculated from the well-known equation  $r = (v_2 - v_1)/(v_2 + v_1)$ . This yields for the ice/sea water boundary a value of  $r = -0.16$ , which produces a distinct reflection for a pulse propagating along the line. The difference with respect to the reflection coefficient given for the pure material is caused by the polyethylene insulation of the strip line which influences the propagation velocity. It follows that an unshielded parallel transmission line frozen into the bottom of an ice shelf can be used as a sensor for the location of the ice/sea water boundary using TDR.

Such a cable would also detect other dielectric changes in a hot-water drilled hole such as frozen water pockets. But an unshielded cable can also pick up noise in the broad-frequency band used by TDR devices. Hence, we chose (for a second drillhole) a combination of a shielded coaxial cable (50 Ω), which is insensitive to its surroundings, down to about 25 m above the ice-shelf bottom followed by the 240 Ω sensor line. Impedance matching between the cables was accomplished by a broad-band RF transformer (type: MCL T4-6). The reflection from this junction serves as a reference level for the determination of travel times.

A problem for the application of the TDR method in ice shelves arises from the absorption losses in the coaxial cable and the strip line, which are frequency-dependent. Values provided by the manufacturer gave absorptions of 5 dB/100 m at 100 MHz for the strip line and 7 dB/100 m at 100 MHz for the coaxial line.

The cables act as low-pass filters which tend to reduce the resolution of the set-up.

We used a Tektronix 1503 TDR cable tester for the generation of a 10 ns half-sine-wave test pulse, sequential sampling and CRT display. Modifications were made in the output module. A 20 MHz quartz reference was used for time calibration. The data were digitally recorded with a Sony digital audio processor PCM-F1 and a Sony video-cassette recorder SL-F1E with a sampling rate of 44 kHz and a 16 bit amplitude resolution. A block diagram of the TDR set-up is shown in Figure 1.

The high digitizing rate of the PCM processor provides an oversampling of the recorded wave form. For practical reasons, the data were reduced to 4096 points by a 215-fold horizontal stack. This process leads to a sample interval of 1.2 ns using a total time window of 5 μs. Since digital-processing techniques allow high precision in phase picking, the onsets of reflections could be determined within one or two samples depending on

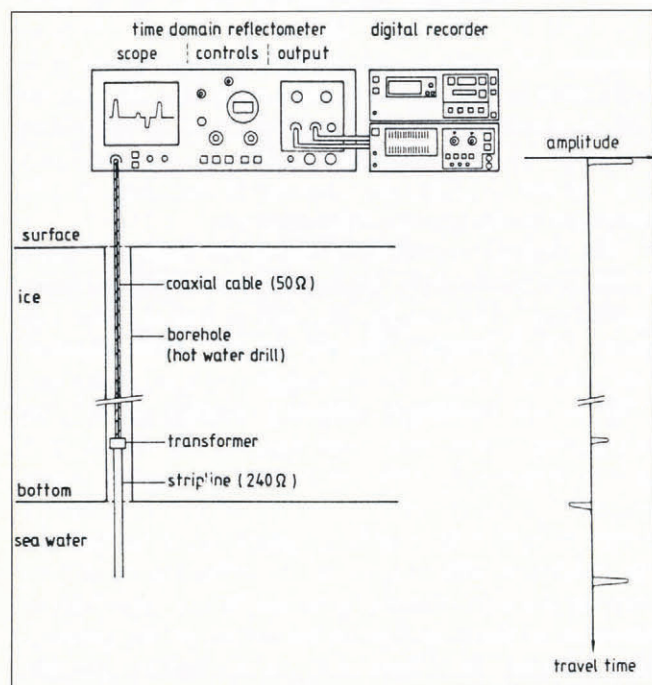


Fig. 1. Block diagram of a TDR set-up with sensor line consisting of coaxial line and strip line.

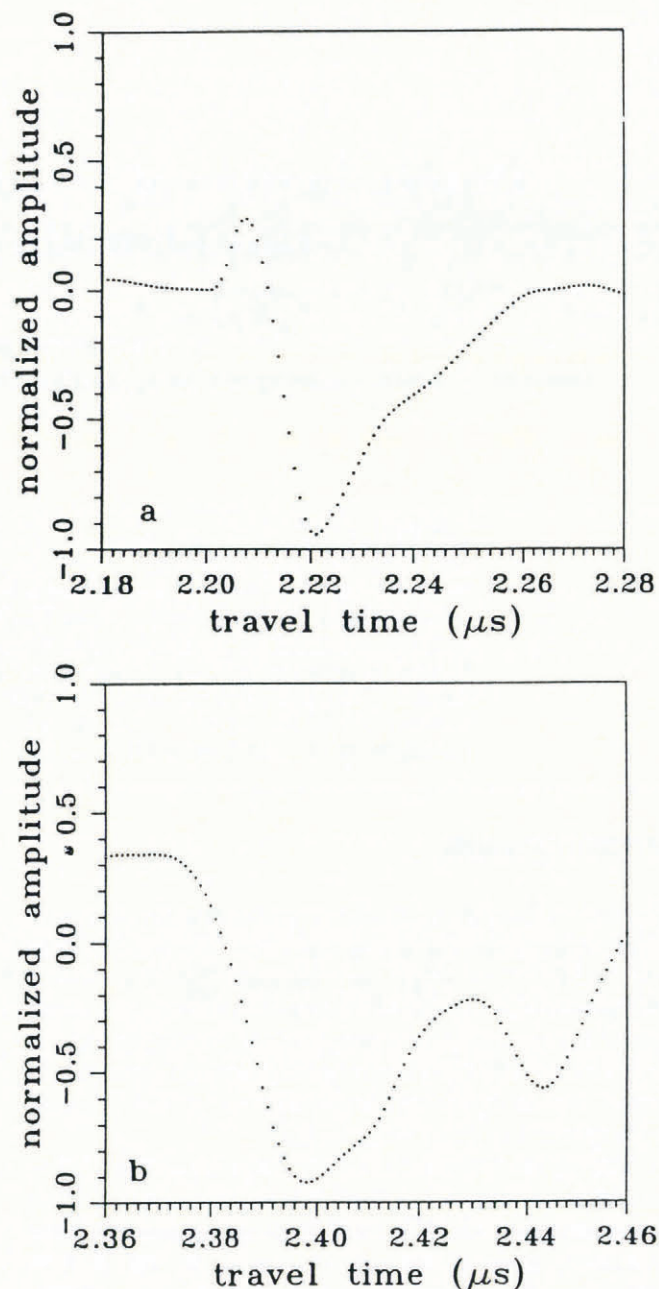


Fig. 2. Digitized recorded wave forms in expanded scale. a. Artificial reflector (RF-transformer). b. Natural boundary ice/sea water.

the reflection coefficient of the boundary. Detailed features of observed reflections are shown in Figure 2a and b.

The determination of travel-time differences and therefore of bottom-melting rates is related to a reference level in definite depth, so time lags inferred by dispersion or frequency-dependent absorption losses of the incident pulse are greatly reduced.

The estimated resolution in ice thickness was calculated as 0.2 using an error in onset picking of two samples and a propagation velocity in ice of 194 m μs<sup>-1</sup>.

### FIELD EXPERIMENTS AND FIRST RESULTS

During the FRIS Expedition 1989–90, two hot-water drill holes had been prepared with different combinations

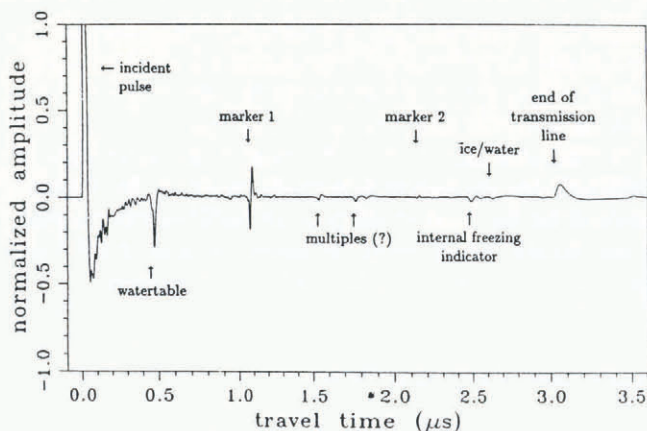


Fig. 3. TDR measurement of a  $240\ \Omega$  strip line installed in the 239 m thick ice shelf, 30 dB amplification.

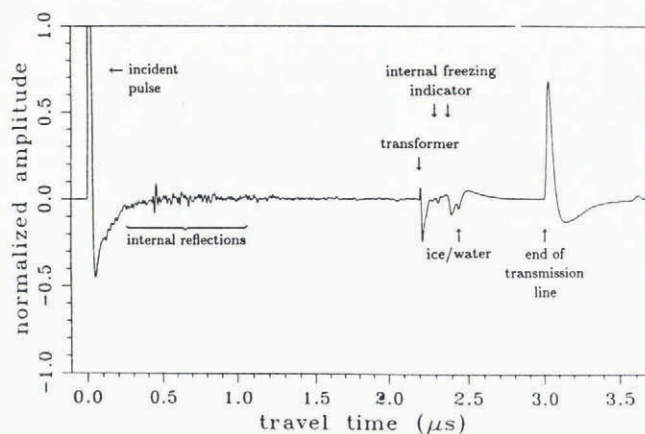


Fig. 4. TDR measurement of a combination of 220 m coaxial line and 60 m of  $240\ \Omega$  strip line installed in the 239 m thick ice shelf, 30 dB amplification.

of TDR sensor lines protruding into the sea water beneath the 239 ( $\pm 2$ ) m thick ice shelf.

The first sensor line we installed was a  $240\ \Omega$  strip line 280 m long. 22 m of the line extended into the sea water, whereas 239 m were influenced by the dielectric properties of the ice shelf. The remaining 19 m were placed on the ice surface. For the determination of reference travel times, two 1 m aluminium stakes were attached to the strip line at distances of 110 and 210 m from its top before lowering the cable down the hole. The dielectric contrast of these stakes produced reflection signals that can be used as reference levels. Another reference level that produced a reflection was the open end of the strip line itself. A TDR measurement of this line is shown in Figure 3.

The measurement shows a sharp positive source pulse followed by a fading negative overshoot amplitude. The first  $1.0\ \mu\text{s}$  of registration time after the source pulse is marked by noise and different reflection signals caused by the increase in ice density and/or water pockets and ice lenses from the hot-water drilling. The first strong reflection, at  $0.466\ \mu\text{s}$  travel time, corresponds to the water table remaining in the borehole after penetration of the ice shelf by hot-water drilling. The reflections at  $1.067$  and  $2.127\ \mu\text{s}$  are produced by the aluminium stakes on the strip line and serve as fixed reference levels with which to compare the reflection from the ice/sea water transition ( $2.612\ \mu\text{s}$ ), as well as the reflection from the end of the sensor line at  $3.017\ \mu\text{s}$ .

The reason for the different signals between  $1.5$  and  $1.9\ \mu\text{s}$  is unknown. Perhaps they can be explained by multiple-reflection signals or by defects in the insulation of the strip line.

The second borehole was prepared with a line consisting of 220 m of coaxial cable and 60 m of  $240\ \Omega$  sensor strip line connected by an RF transformer. Figure 4 shows an example of a measurement with this arrangement.

Because the first 220 m of cable are shielded, the time interval up to  $2.2\ \mu\text{s}$  after the source pulse is not influenced by its surrounding material. The appearance of high-amplitude noise during the first  $1.5\ \mu\text{s}$  of registration may be the result of a relatively large amplification (30 dB) and lower absorption losses. The

first detectable reflection is caused by the RF transformer after a travel time of  $2.202\ \mu\text{s}$ . The distinct reflection with reversed phase at  $2.431\ \mu\text{s}$  corresponds to the ice/sea water boundary. The negative reflection coefficient from this boundary produces the phase inversion. Superposed on this reflection are other signals that result from internal freezing processes in the drillhole. The signal from the end of the strip line shows a strong positive amplitude at  $2.997\ \mu\text{s}$ .

Signals with this configuration of sensor line are larger than those with the unshielded strip line, even if the impedance mismatch of the strip line is taken into account. We infer that the attenuation of the unshielded line must be strongly influenced by the surrounding material, i.e. there is a stronger attenuation in the strip line surrounded by ice than in the coaxial cable, since manufacturer's data show larger absorption losses in the coaxial line than in the strip line.

## DISCUSSION AND CONCLUSION

The results of our measurements on transmission lines as sensors for dielectric contrasts in ice shelves, especially the ice/sea water boundary, were quite encouraging, although a melting rate for this location could not be determined from the data of the 1989–90 season for two reasons:

From temperature measurements, we knew that refreezing of the drillhole at the ice-shelf bottom occurs for about 20 d after drilling. Figure 5 shows the temperature evolution of a neighboring borehole in the lowest 8 m to demonstrate the refreezing process. Temperature element No. 64 was placed close to the ice-shelf bottom in the sea water and shows an almost constant value for the registration period. Elements Nos 63–60 were placed near the ice-shelf bottom with a spacing of about 2 m. The temperature record shows that the refreezing of the borehole near the bottom (No. 63) took place between the fifteenth and twentieth days after drilling. The maximum cooling rate occurs at that time, when liquid water is no longer present. The temperature increase recorded by the other three elements during the first 5 d may be due to

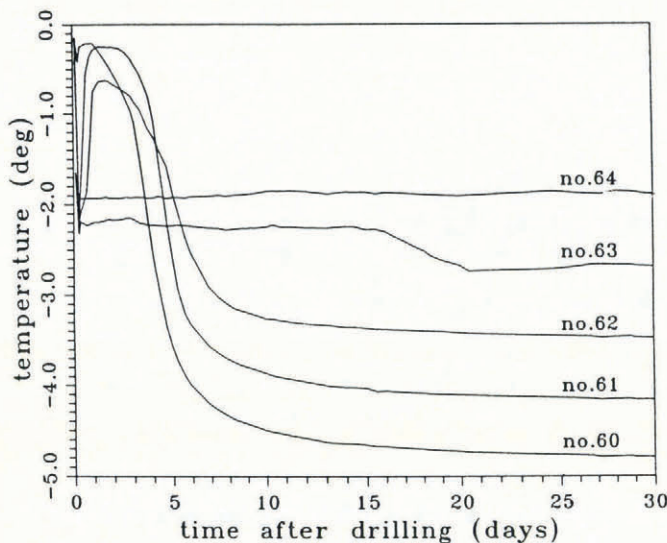


Fig. 5. Refreezing process of a 239 m deep melt hole in the lowest 8 m. Measurement with Pt100 elements at a spacing of about 2 m. Element No. 64 was placed close to the ice-shelf bottom in the sea water.

crystallization heat of undercooled sea water, which penetrates into the borehole, so the time periods of 18 and 21 d, respectively, for the TDR measurement with both configurations was too short, compared with the time period of 20 d needed to refreeze the lower part of the borehole, in order to detect travel-time differences and calculate bottom-melting rates.

Another problem arises from the refreezing. Since the lowest 8 m of the borehole was possibly influenced by saline sea water, the refreezing of the borehole may have taken place by the formation of frazil ice at a rate that depends on the salt content. This process would form relatively porous sea ice with brine pockets (Buynitzkiy, 1967). The reflection coefficient for electro-magnetic waves in this complex mixture at a sea-water boundary would generally be different from that at a boundary between glacier ice and sea water. We suppose that it takes a long time to refreeze the lowest few meters of the borehole to form compact pure ice down to the bottom of the ice shelf, so that a distinct reflection signal of that boundary can be obtained. We observed that the reflected signal from the ice/sea water boundary is characterized by multiple wave forms that change their phase and amplitudes with time, presumably as the refreezing process continues.

Besides the fact that refreezing takes rather a long time, the basal-melting rate itself defines the necessary period for its determination with a given accuracy. In the case of our drill site, the bottom-melting rate was calculated from the continuity equation for mass conservation under the assumption of steady state as  $1.5 \pm 0.15 \text{ m a}^{-1}$  (Determann and others, 1991). This means a melting rate of  $0.004 \text{ m d}^{-1}$  and a period of 50 d

to observe a melting of 0.2 m with our TDR system. From the system resolution, it follows that a period of more than 1 year is necessary to obtain a measurement of the basal-melting rate with an error of 10% or less.

Summarizing, it can be said that time-domain reflectometry measurements could prove to be a useful method for the measurement of ice-shelf bottom melting, if the sensor line is properly frozen in and if the time interval for re-measuring the line is long enough.

## ACKNOWLEDGEMENTS

Thanks are due to F. Thyssen for initiating this project and for helpful discussions, and L. Hempel for his active assistance in the field work. We also thank C.R. Bentley and an anonymous reviewer for constructive comments and helpful suggestions on the manuscript. Funding by the Deutsche Forschungsgemeinschaft (DFG, Th168/20-2) and logistic support by the Alfred-Wegener-Institut für Polar- und Meeresforschung are gratefully acknowledged.

## REFERENCES

- Blindow, N., P. Ergenzinger, H. Pahls, H. Scholz and F. Thyssen. 1987. Continuous profiling of subsurface structures and groundwater surface by EMR methods in southern Egypt. *Berliner Geowissenschaftliche Abhandlungen, Reihe A* 75.2, 575–628.
- Buynitzkiy, V. Kh. 1967. Structure, principal properties, and strength of Antarctic sea ice. *Sov. Antarct. Exped. Inf. Bull.*, 6(6), 504–510.
- Crary, A. P., E. S. Robinson, H. F. Bennett and W. W. Boyd, Jr. 1962. Glaciological regime of the Ross Ice Shelf. *J. Geophys. Res.*, 67(7), 2791–2807.
- Determann, J., K. Grosfeld and B. Ritter. 1991. Melting rates at the bottom of Filchner-Ronne Ice Shelf, Antarctica, from short-term mass-balance studies. *Polarforschung*, 60(1), 1990, 25–32.
- Morey, R. M., A. Kovacs and G. F. N. Cox. 1984. Electromagnetic properties of sea ice. *CRREL Rep.* 84–2.
- Thyssen, F. 1988. Special aspects of the central part of Filchner-Ronne Ice Shelf, Antarctica. *Ann. Glaciol.*, 11, 173–179.
- Topp, G. C., J. L. Davis and A. P. Annan. 1982a. Electromagnetic determination of soil water content using TDR: I. Applications to wetting fronts and steep gradients. *Soil Sci. Soc. Am. J.*, 46, 672–678.
- Topp, G. C., J. L. Davis and A. P. Annan. 1982b. Electromagnetic determination of soil water content using TDR: II. Evaluation of installation and configuration of parallel transmission lines. *Soil Sci. Soc. Am. J.*, 46, 678–684.

*The accuracy of references in the text and in this list is the responsibility of the authors, to whom queries should be addressed.*